

黑龙江省三江盆地鹤岗凹陷下白垩统猴石沟组沉积特征

冀华丽¹⁾, 何中波¹⁾, 秦明宽¹⁾, 卫三元¹⁾, 曹建辉¹⁾, 杨帆²⁾

1) 核工业北京地质研究院, 北京, 100029; 2) 中石化石油工程技术研究院, 北京, 100101

内容提要:笔者等通过对鹤岗凹陷北部露头和钻孔资料的综合利用,结合少量的样品分析及薄片鉴定工作,对研究区下白垩统猴石沟组主要岩石学特征、沉积相类型及展布特征进行了综合研究,在此基础上,以砂岩型铀矿成矿理论为指导,对猴石沟组有利成矿砂体的沉积相类型进行了初步讨论。认为①猴石沟组砂体以长石岩屑砂岩和岩屑砂岩为主,主要为陆相淡水沉积环境,具较高的还原容量;②研究区内猴石沟组主要为扇三角洲沉积环境,并划分为辫状河道、漫滩沼泽、水下分流河道、河口坝、席状砂和分流间湾等6种微相;③猴石沟组沉积辫状河道砂体可作为寻找潜水氧化带型砂岩型铀矿的重点类型,而水下分流河道砂体是作为寻找层间氧化带型砂岩型铀矿的主攻类型。

关键词:下白垩统猴石沟组;扇三角洲;沉积相;鹤岗凹陷

鹤岗凹陷是黑龙江省东部三江盆地的次级构造单元,位于三江盆地与小兴安岭东坡接触部位,是我国东北地区重要及主要的中新生代产煤盆地之一(温泉波等,2008;方石等,2012;张兴洲等,2015;蔡超等,2016;何中波等,2018a)。研究区最早的地质工作可追溯到解放前,长期以来石油及煤田部门在该地区开展了大量的基础地质及煤田地质工作,尤其是在盆地的性质、构造演化、含煤层沉积环境及其演化特征等方面取得了大量的研究成果(侯伟等,2007;许仔明等,2010;季汉成等,2013;刘孟骐等,2017)。前人研究较多的是对主要含煤地层下白垩统城子河组(K_1c)和穆棱组(K_1m)沉积环境、聚煤条件及其沉积后经历的改造作用进行了研究(杨子荣等,1997;李纯杰等,2010;程三友等,2012;陈东旭,2016),而对下白垩统猴石沟组的研究较少,尤其是关于猴石沟组沉积特征未见在公开文献中论述。近年来,随着我国北方盆地砂岩型铀矿找矿工作的持续开展,作为我国北方中新生代产煤盆地的鹤岗凹陷越来越受到铀矿地质工作者的关注(陈戴生等,2003;张金带等,2010;蔡煜琦等,2015;李子颖等,2015;何中波等,2016;秦明宽等,2017;Qin

Mingkuan et al., 2018),尤其是在研究区下白垩统猴石沟组(K_1h)发现了较好的砂岩型铀矿找矿线索,但是关于该组的砂体发育特征及沉积体系发育特征研究较为薄弱,制约了该盆地铀矿勘查工作的开展。本文从沉积学角度出发,对研究区下白垩统猴石沟组(K_1h)砂体类型及沉积相展布特征进行了综合研究,对研究区砂岩型铀矿找矿工作具有一定的指导意义。

1 区域地质背景

研究区地理上属于黑龙江省的东北部,大地构造上处中亚造山带的东段和西太平洋构造带交结复合部位。中生代以来,受蒙古—鄂霍茨克洋自西向东剪刀式的闭合和古太平洋板块持续的俯冲作用,在佳木斯地块、那丹哈达岭地块、小兴安岭—张广才岭地块、兴凯地块及牡丹江断裂、依兰舒兰断裂等先存构造基础上形成了包括鹤岗凹陷在内的三江盆地及黑龙江东部盆地群。研究区西缘受牡丹江断裂控制,东南缘有依兰—伊通断裂带西缘断裂所截切。由于西侧小鹤立河断裂及东侧的鸭蛋河断裂同生构造控制,使鹤岗凹陷呈长箕状(图1;和钟铧等,

注:本文为国防预研究基金和中国核工业地质局铀矿勘查项目(编号:201713,201929)的共同成果。

收稿日期:2019-06-05;改回日期:2019-09-18;责任编辑:刘志强。Doi: 10.16509/j.georeview.2020.01.004

作者简介:冀华丽,女,1989年生,工程师,硕士,矿产普查与勘探专业,主要从事沉积盆地分析及砂岩型铀矿成矿条件研究工作;Email:jhl19890303@163.com。通讯作者:何中波,男,1980年生,高级工程师,主要从事盆地分析、砂岩型铀矿成矿条件、成矿机理及成矿预测研究工作;Email:hzb100029@163.com。

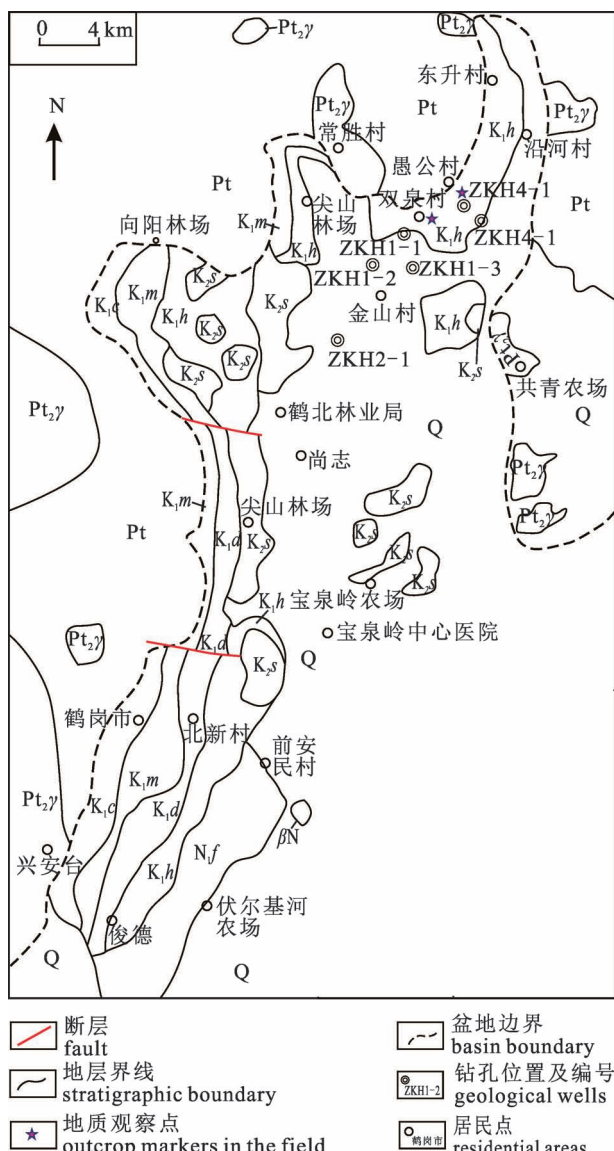


图1 黑龙江省三江盆地鹤岗凹陷构造位置

Fig. 1 Tectonic position of the Hegang Depression,
Sanjiang Basin in Heilongjiang Province

Q—第四系; N₁f—新近系富锦组; K₂s—上白垩统松木河组;
K₁h—下白垩统猴石沟组; K₁d—下白垩统东山组; K₁m—下白垩统穆棱组; K₁c—下白垩统城子河组; Pt—元古宇变质岩;
Pt₂γ—中元古代花岗岩

Q—Quaternary; N₁f—Neogene Fujin Formation; K₂s—Upper Cretaceous Songmuhe Formation; K₁h—Lower Cretaceous Houzhigou Formation; K₁d—Lower Cretaceous Dongshan Formation; K₁m—Lower Cretaceous Muling Formation; K₁c—Lower Cretaceous Chenzihe Formation; Pt—Proterozoic metamorphic rocks; Pt₂γ—Mesoproterozoic granite

2008; 梁奉奎等, 2011; 廖群山等, 2011)。

盆地基底主要由前古生界麻山群、黑龙江群深变质岩系及元古宙混合花岗岩、华力西期花岗岩等

共同组成(贾承造等, 2010; 张云鹏等, 2016; 张君峰等, 2018)。沉积盖层以白垩系为主: 主要有下白垩统城子河组、穆棱组、东山组、猴石沟组, 上白垩统松木河组, 古近系宝泉岭组和新近系富锦组, 总厚度大约3100 m(图2)。其中, 城子河组和穆棱组属陆相含煤碎屑岩建造, 下白垩统东山组和上白垩统松木河组为陆相火山碎屑—火山岩建造, 目标层下白垩统猴石沟组为一套正常沉积的碎屑岩建造, 是盆地断—拗转换期的沉积产物。

2 沉积特征

2.1 砂岩岩石学特征

笔者等对多次采取的样品进行了镜下观察分析, 对砂岩的成分、结构及砂岩所反映的大地构造性质进行了探索性研究。镜下观察统计表明, 目的层猴石沟组砂岩碎屑颗粒主要为石英、长石和岩屑, 岩屑种类丰富, 以花岗岩和变质岩岩屑为主, 以及少量的板岩和片岩。

笔者等对愚公村—双泉村—共青城地区目的层猴石沟组砂岩45块样品, 进行了镜下观察和碎屑颗粒的分析统计, 样品取样钻孔分别为ZKH1-1、ZKH1-2、ZKH1-3、ZKH2-1、ZKH4-1和ZKH4-2(图1), 采用了曾允孚(1986)的砂岩分类方法, 在(Q—F—R)三元图上进行投图(图3)。从图中可以看出, 鹤岗凹陷愚公村—双泉村—共青城地区砂岩类型主要为长石岩屑砂岩和岩屑砂岩。

通过样品的镜下观察分析, 对砂岩成分、结构进行了研究。显微镜观察统计表明, 猴石沟组砂岩碎屑成份以石英、长石和岩屑为主, 其次为云母类矿物及少量重矿物。石英含量约在20%~45%, 以次棱—次圆状居多(图4a)。石英碎屑既有单晶的, 又有双晶的。多数单晶石英表面干净, 无波状消光, 少量具有带状消光的石英碎屑, 少量颗粒具边部熔蚀结构。可见石英集合体, 呈不均匀消光(图4b)。长石的含量比石英少, 平均含量在10%~35%, 有钾长石和斜长石, 多数以斜长石为主, 其中钾长石多无条纹、无格子双晶, 少见有棋盘格子交代产生的碱性长石假象, 斜长石常见钠长双晶和聚片双晶(图4c)。多数长石蚀变明显, 主要由粘土化(高龄石化)、水云母、绢云母化(图4d), 部分颗粒表面被铁染(图4e)。岩屑组份含量极为丰富, 成份复杂, 含量约在35%~65%, 成份以变质岩岩屑为主, 少量火山和沉积岩屑。岩屑岩性以凝灰岩、中酸性火山岩、花岗岩、变质砂岩为主, 少量云母石英片岩、云母片岩和

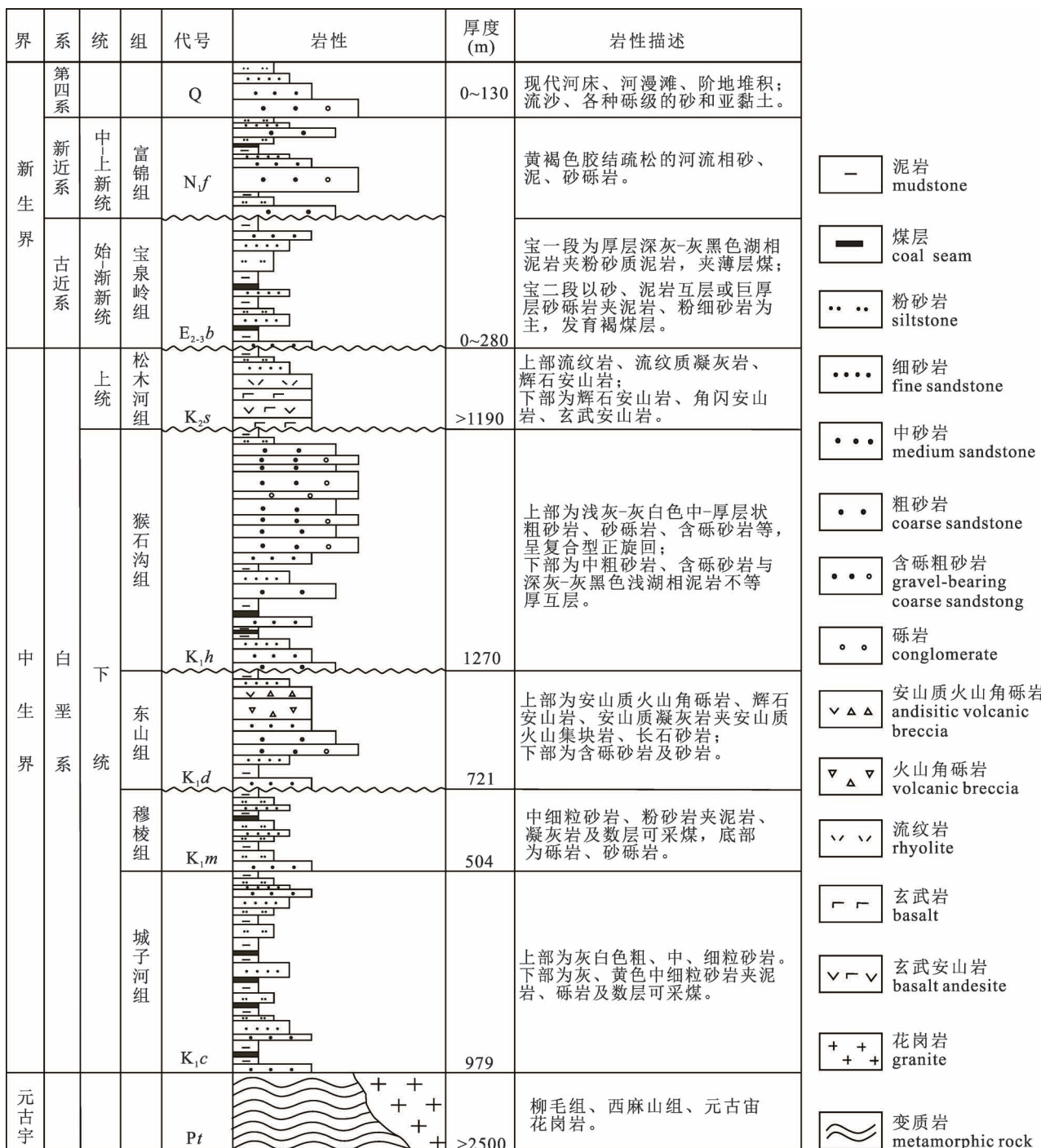


图 2 三江盆地鹤岗凹陷综合地层柱状图

Fig. 2 Comprehensive stratigraphic column of the Hegang Depression in Sanjiang Basin

千枚岩。云母含量变化较大,一般占碎屑含量的2%~5%,主要为黑云母,其次为白云母,多因压实作用折曲变形(图4f)。重矿物含量约占碎屑含量的1%,其成份主要为锆石、金红石、电气石、绿帘石、以及钛铁矿、独居石。除此之外,还含有少量有机质和金属矿物。有机质以植物茎秆、炭化植物碎

屑和炭屑形式存在。金属矿物则以黄铁矿和钛铁矿为主,分布于矿物溶蚀孔和粒间胶结物中,多呈星点状、浸染状,集合体呈胶状、团块状产出,并遭受不同程度的氧化作用,形成褐铁矿。

2.2 微量元素特征及环境意义

沉积盆地具有基本的地球化学环境,对元素的

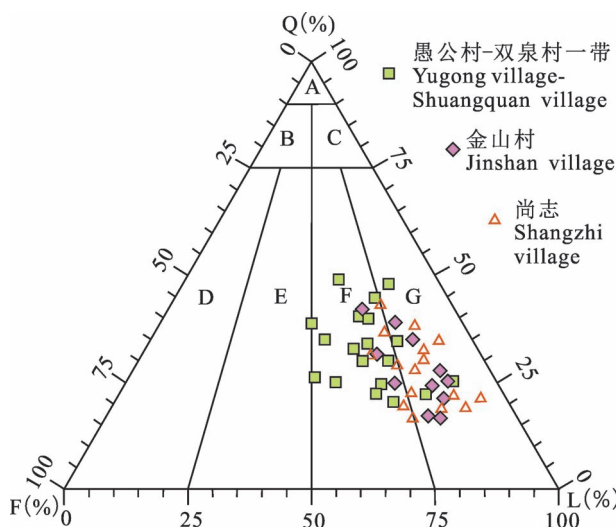


图3 三江盆地鹤岗凹陷愚公村—双泉村—金山村—尚志地区猴石沟组砂岩分类

Fig. 3 The sandstone types of the Houshigou Formation in Yugongcun—Shuangquancun—Jinshancun—Shangzhi area, the Hegang Depression, Sanjiang Basin

A—石英砂岩; B—长石石英砂岩; C—岩屑石英砂岩; D—长石砂岩; E—岩屑长石砂岩; F—长石岩屑砂岩; G—岩屑砂岩
A—Quartz sandstone; B—feldspathic quartz sandstone; C—lithic quartz sandstone; D—feldspar sandstone; E—lithic feldspar sandstone; F—feldspar lithic sandstone; G—lithic sandstone

分布起控制作用,且表现出元素分布的规律性。因此可通过研究某些特征元素含量及其比值来识别沉积环境(Lermana et al., 1978; Bhatia, 1983; Bhatia et

al., 1986; Riboulleau et al., 2003; Rimmer et al., 2004; Algeo et al., 2004)。

笔者等对鹤岗凹陷钻孔 ZKH1-1、ZKH1-2、ZKH1-2、ZKH4-1 和 ZKH4-2 猴石沟组 26 块泥岩样品微量元素进行测定,并与 Hatch 和 Leventhal (1992) 建立的 $V/(V+Ni)$ 值反映氧化还原特性的指标进行对比, $V/(V+Ni)$ 值通常用于判断沉积物沉

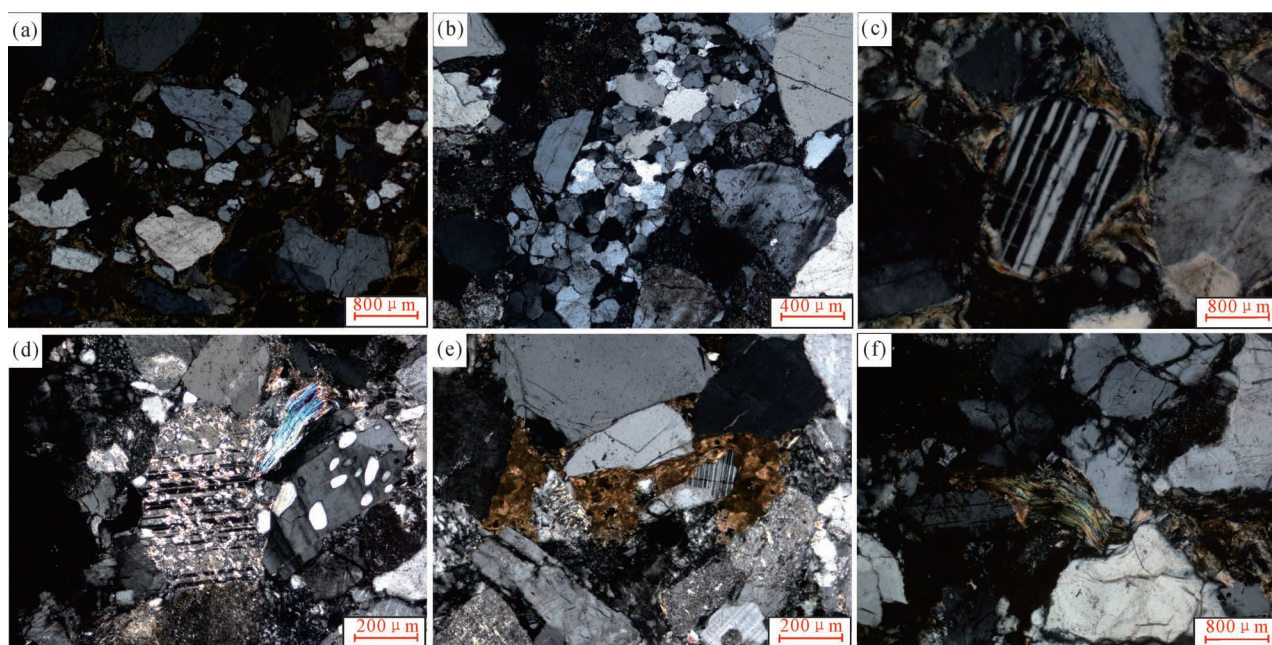


图4 三江盆地鹤岗凹陷愚公村—双泉村地区目的层砂岩显微特征

Fig. 4 Microscopic characteristics of the target layers of Yugongcun—Shuangquancun area of the Hegang Depression in the Sanjiang Basin

- (a) 不等粒长石岩屑砂岩(次棱角状,孔隙胶结,ZKH4-1-12 号样,212.53 m (+), $\times 100$); (b) 石英集合体,呈不均匀消光(ZKH1-2-18 号样,341.87 m (+), $\times 100$); (c) 聚片双晶斜长石(ZKH1-1-08 号样,261.38 m (+), $\times 100$); (d) 斜长石绢云母化(ZKH2-1-11 号样,196.37 m (+), $\times 100$); (e) 杂基被铁染(ZKH4-2-25 号样,319.65 m (+), $\times 100$); (f) 云母类矿物压实弯曲变形,且具定向排列(ZKH1-3-07 号样,193.45 m (+), $\times 100$)
(a) Inequigranular feldspar lithic sandstone (subangular, pore cementation, sample number ZKH4-1-12, 212.53 m (+), $\times 100$); (b) quartz aggregates with inhomogeneous extinction (sample number ZKH1-2-18, 341.87 m (+), $\times 100$); (c) polymeric bicrystalline plagioclase (sample number ZKH1-1-08, 261.38 m (+), $\times 100$); (d) plagioclase sericitization (sample number ZKH2-1-11, 196.37 m (+), $\times 100$); (e) heterogeneous groups stained with iron (sample number ZKH4-2-25, 319.65 m (+), $\times 100$); (f) mica minerals are compacted, bent and aligned (sample number ZKH1-3-07, 193.45 m (+), $\times 100$)

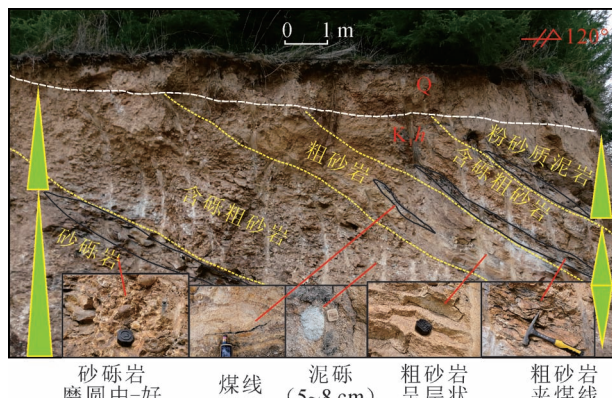


图 5 三江盆地鹤岗凹陷双泉村猴石沟组野外露头特征
Fig. 5 Outcrop characteristics of the Houshigou Formation in Shuangquan village, the Hegang Depression, Sanjiang Basin

积时底层水体分层强弱(Hatch and Leventhal, 1992; 熊国庆等, 2008), 高于 0.84 分层强, 0.60~0.84 之间分层中等, 0.4~0.6 之间分层弱。

本研究区内 15 件样品的 $V/(V+Ni)$ 值在 0.60~0.82 之间起伏波动, 另外 11 件样品的 $V/(V+Ni)$ 值在 0.82~0.93, 这说明研究区猴石沟组湖盆水体分层性中等到强, 可推断研究区在猴石沟组沉积时期为中等到强烈的厌氧还原环境。另外国外研究认为(邓宏文等, 1993; Rimmer et al., 2004; Scheffler et al., 2006; Tribouillard et al., 2006; 陶树等, 2009; 范玉海等, 2012; 张天福等, 2016), 海水中 Ni 的含量大于 40×10^{-6} , 而淡水中一般不高于 30×10^{-6} 。研究区 Ni 的含量均小于 30×10^{-6} , 表明研究区应不是海相沉积, 而是陆相淡水半咸化环境。

2.3 野外露头沉积特征

以双泉村和愚公村剖面(剖面位置见图 1)为例, 该剖面地理位置位于鹤北镇双泉村和愚公村。从双泉村野外露头(图 5)分析来看, 猴石沟组自下而上主要由浅黄—灰黄色砂砾岩、粗砂岩和粉砂质泥岩组成, 夹多层煤线和煤层。沉积物总体具有粒度粗(平均 0.25~2.00 mm)、厚度大(单层厚度平均 1~6 m)沉积特征, 分析认为具有典型的河道沉积特征, 垂向上多个间断性正韵律叠置, 层内平行层理、中型槽状交错层理发育, 砂砾层厚度一般 5~10 m, 主要为砾岩、含砾粗砂岩沉积, 底部可见滞留砾石(20~55 mm)沉积, 砾石分选中—差, 砾径多在 10~30 mm, 多次棱角一次圆状, 成分以石英、燧石为主, 反映了沉积时水动力较强、沉积物供给较快的沉积特征。



图 6 三江盆地鹤岗凹陷愚公村猴石沟组野外露头特征
Fig. 6 Outcrop characteristics of the Houshigou Formation in Yugong village, the Hegang Depression, Sanjiang Basin

愚公村附近农田的河谷露头出露较好, 该剖面绵延长约 1 km, 厚约十余米。从愚公村野外露头剖面(图 6)可观察到, 猴石沟组粗砂岩厚度大, 分布稳定。整体为中—厚层状的灰—灰黄—浅黄色粗砂岩夹薄层灰色粉细砂岩、泥质粉砂岩(图 7a), 砂岩中富煤线, 偶含砾石(6~12 mm), 砾石磨圆较好, 砂体胶结疏松, 成岩度低, 透水性好。砂岩层间隙发育裂隙面, 被褐铁矿化, 呈褐黄色。砂岩底部发育冲刷面, 可见硕大泥砾(50~80 mm), 反映了河道沉积特征; 煤层与褐黄色粗砂岩呈渐变接触, 多为褐煤或半暗煤, 厚度约 0.1~1.5 m, 厚者可达 2 余米, 常夹透镜状粗砂岩, 推断为冲积平原上的沼泽发育地带。

3 沉积相分析

3.1 沉积相类型

3.1.1 扇三角洲

扇三角洲是以冲积扇为供源沉积到水体的结果, 一般至少在近端保留有陆上部分(吴崇筠, 1986; 中国石油学会石油地质委员会, 1988)。是一种粗碎屑带状体, 向盆地中心方向与湖泊沉积呈指状交互, 局部含炭质泥岩或薄煤层。研究区内主要发育扇三角洲平原亚相和前缘亚相, 进一步的微相划分如下:

(1) 扇三角洲平原亚相: 扇三角洲平原亚相为扇三角洲沉积的陆上部分, 以沉积物重力流为主的粗粒沉积物为特征, 砂砾互层, 具不明显的平行层理或交错层理, 分选差, 具砂质基质, 反映了粗碎屑砂砾岩沉积的陆上冲积和浅水氧化环境的岩性特征。发育辫状河道和漫滩沼泽 2 种微相。(① 辫状河道:

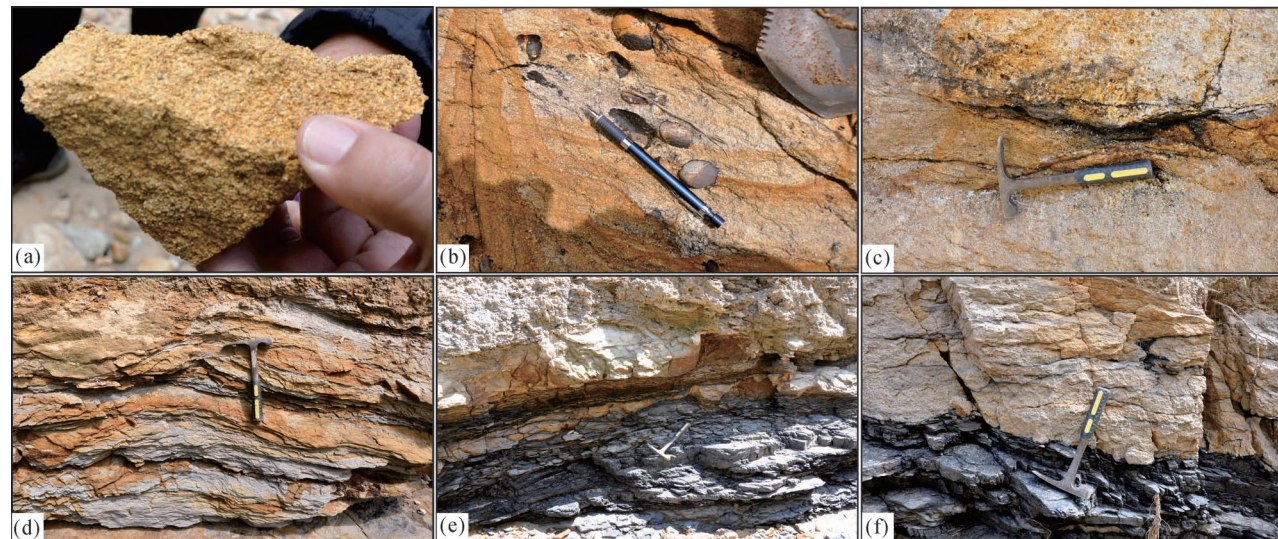


图 7 三江盆地鹤岗凹陷猴石沟组典型沉积构造特征

Fig. 7 Typical sedimentary structure characteristics of the Houshigou Formation in the Hegang Depression, Sanjiang Basin
 (a) 灰黄色粗砂岩, 胶结疏松; (b) 灰黄色粗砂岩含砾石; (c) 灰黄色粗砂岩夹煤线; (d) 灰—灰黄色粉砂岩与深灰色泥岩薄互层;
 (e) 透镜状煤层与上部砂岩层渐变接触; (f) 透镜状煤层与上部砂岩层突变接触

(a) grayish yellow coarse sandstone, Loose cementation; (b) gravel-bearing grayish yellow coarse sandstone; (c) grayish yellow coarse sandstone coal line; (d) thin interbedding of grey—grayish yellow siltstone and dark grey mudstone; (e) gradual contact between lenticular coal seam and upper sandstone; (f) abrupt contact between lenticular coal seam and upper sandstone seam

岩性主要为灰—灰黄色砂砾岩、含砾粗砂岩、含砾中砂岩、细砂岩等组成, 夹厚层粉砂质泥岩, 砂岩中富煤线(图 7a,b)。整体以砂砾岩和粗砂岩沉积为主、成熟度低, 砾石大小一般多 2~40 mm, 最大可达 60 mm, 呈次棱角状—次圆状(图 7c), 以颗粒支撑为主, 也有部分基质支撑, 砾石成分主要为硅质岩、变质岩岩屑, 颜色多样。粗碎屑沉积中常见冲刷—充填构造, 主要发育正粒序层理、波状层理、块状层理。垂向上, 表现为多期砾质河道沉积叠置而成, 自下而上为多个由粗至细的正韵律旋回组成, 单次河道充填厚度一般为 1~25 m, 测井曲线呈钟形或箱形(图 8)。以重力流成因的沉积构造, 砂砾岩大小混杂, 分布不均, 递变层理发育。②漫滩沼泽: 发育于陆上辫状河道间的低洼地, 为洪水期漫越河道所形成于两侧的细粒物质, 由于排水不良, 为一停滞的还原环境。其沉积为深色粉砂质泥岩、泥炭、褐煤(图 7d), 褐煤层与上下部砂岩多呈渐变接触, 有的呈突变接触(图 7e, f), 测井曲线表现为中—高幅微锯齿状指形。

(2) 扇三角洲前缘亚相: 扇三角洲前缘亚相为扇三角洲沉积的水下部分, 主要发育水下分流河道、河口砂坝、席状砂和分流间湾沉积。①水下分流河道: 是水上辫状河道在水下的延伸, 是扇三角洲前缘

沉积的主体, 其沉积特征与水上辫状河道相似, 只是水动力稍弱, 水下分流河道沉积物的碎屑粒度随分支叉河道的水下延伸而变细、层状增厚。岩性主要由中—厚层灰—灰白色含砾粗砂岩和砂砾岩组成, 夹深灰—灰黑色含砾粉砂质泥岩, 富含煤线和炭屑。砂体底面常见冲刷界面并伴有撕裂泥屑(图 9a), 底部常见块状层理、平行层理至大中型槽状交错层理等牵引流成因沉积构造(图 9b、图 10)。另外, 砂层之间常夹薄层泥岩, 多个砂岩层、砂砾岩层叠置可达数十米厚, 局部可见正反粒序, 厚层砂体的测井曲线多呈齿化钟形(图 10); 砾石具有重力滑动剪切成因的滑动面(图 9c)以及伴生的砾石定向特征、具有很好的磨圆度, 颗粒支撑, 板条状砾石具定向性, 发育砂岩透镜体, 具有较好成层性。②河口坝(前缘滩坝): 位于水下分流河道的前缘和侧缘, 是由于水体深度的增加或地形坡降突然变缓, 水下分流河道带来的碎屑物质在河道前缘沉积下来所形成的向上变粗的反粒序砂坝。下部为中—薄层泥质粉砂岩或粉砂质泥, 发育水平层理、波状层理(图 11), 中上部为厚层、块状细砂岩和中砂岩, 发育斜层理和交错层理, 测井曲线往往呈中—高幅漏斗形。③席状砂: 分布在河口坝外缘的薄层砂体, 源于河口坝砂体受波浪和岸流淘洗、簸选, 发生侧向迁移。主要为中

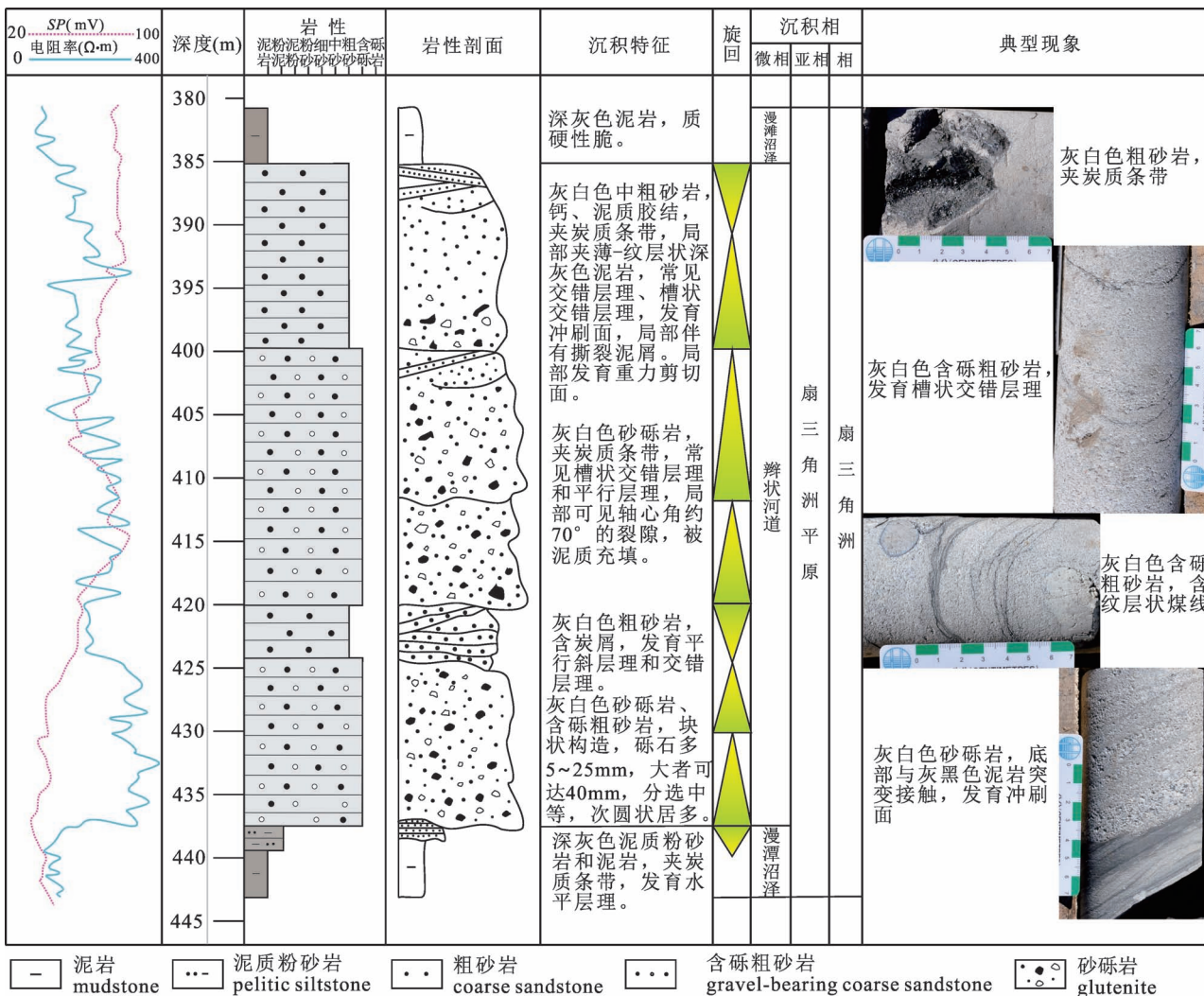


图 8 三江盆地鹤岗凹陷愚公村钻孔 ZKH4-2 猴石沟组 381.25~443.50 m 段扇三角洲平原沉积序列

Fig. 8 Depositional sequence of fan delta plain at 381.25~443.50 m of the Houshigou Formation from Well ZKH4-2 in Yugong village, the Hegang Depression, Sanjiang Basin

薄层杂色砾岩层和灰白色砂岩的不等厚互层。砾岩层富含泥砾和碳屑, 砾石成分复杂, 具块状构造、反—正粒序(图 9d);发育波状交错层理(图 9e), 砾石杂基以灰绿色为主, 分选较好, 颗粒支撑, 孔隙式胶结。自然电位曲线和双侧向曲线呈中低幅齿化指形。席状砂单层厚度一般大于 0.5 m, 横向上增厚或变薄, 但延伸相对较为稳定。④分流间湾:是洪水期间沉积物从水下分流河道中溢到河道间沉积而形成, 其局部与浅湖相通, 沉积作用以悬浮沉积为主。河道间漫流沉积的粉砂和泥质物, 可以充当良好隔水层, 常与水下分流河道砂体组合, 形成“泥—砂—泥”结构, 岩性主要为暗色块状泥岩、粉砂质泥岩、泥质粉砂岩和粉砂岩, 并含炭化植物茎秆化石。单层厚度 1.5~5.0 m, 横向分布不稳定, 测井曲线为低

幅齿形。

3.1.2 滨浅湖

岩性主要为深灰—灰黑色粉砂质泥岩和泥岩, 可见爬升沙纹层理、水平层理, 还可见少量虫孔(图 9f、g、h、i)。灰黑色泥岩断面发育保存完整的各种类型的植物化石, 粗大的炭化茎秆化石依然可辨其纹理结构, 竹叶状叶片化石栩栩如生(图 12a、b), 另外砂岩中亦可见丰富的煤线和炭质条带(图 12c、d), 说明了植屑发育的密集程度, 亦从侧面反映了猴石沟组沉积时期, 具有较高的还原容量。

3.2 沉积序列演化特征

沉积序列可在一定程度上可反映岩性组合特征和沉积环境。研究区猴石沟组自下而上经历了滨浅湖—扇三角洲前缘—扇三角洲平原的环境变化。由

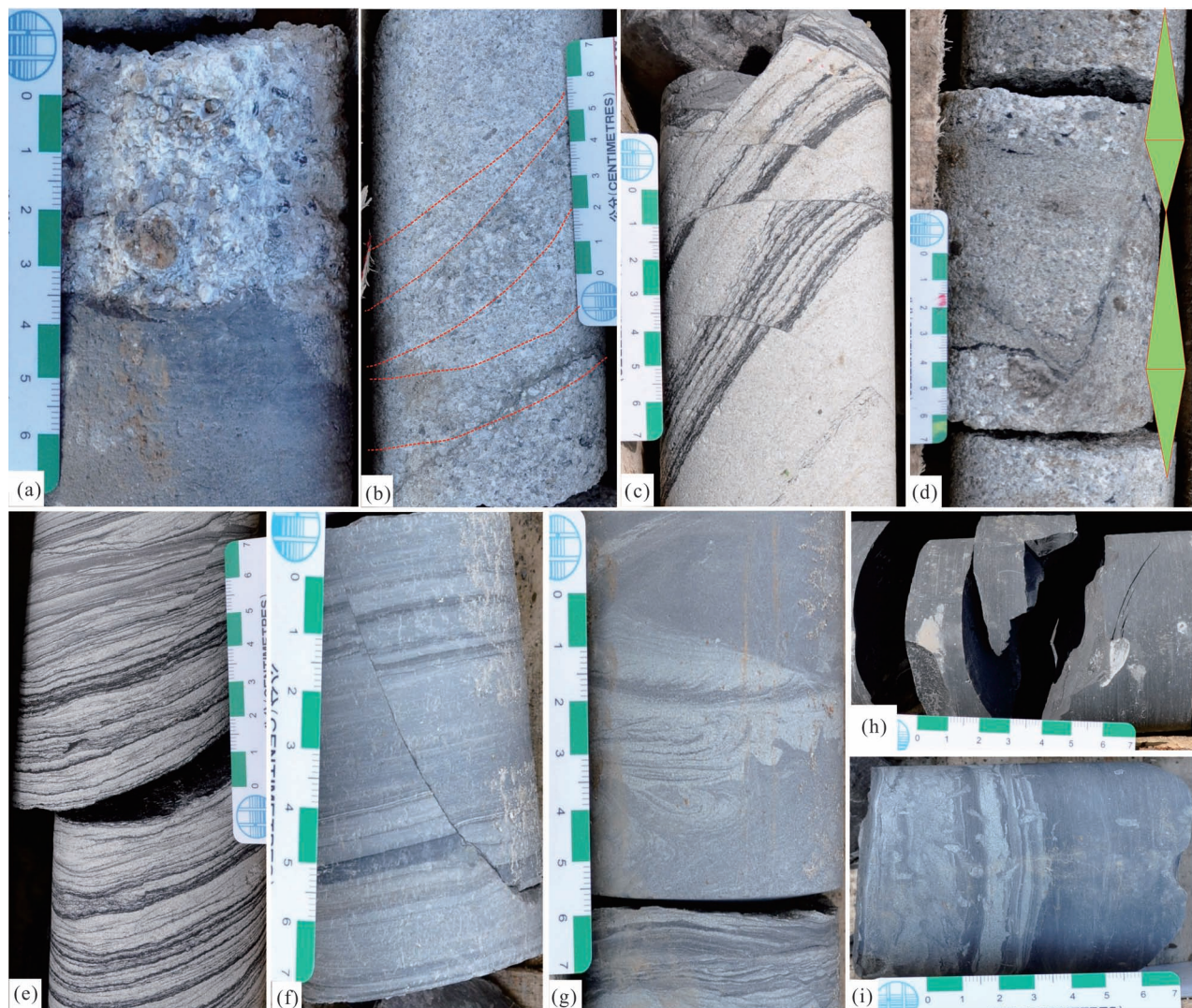


图9 三江盆地鹤岗凹陷猴石沟组岩芯特征

Fig. 9 Characteristics of the cores from the Houshigou Formation in the Hegang Depression, Sanjiang Basin

(a) 钻孔 ZKH1-2, 241.29 m, 灰白色砂砾岩与湖相泥岩突变接触, 发育冲刷面; (b) ZKH4-2, 189.83 m, 灰白色含砾粗砂岩, 发育槽状交错层理; (c) 钻孔 ZKH1-1, 296.35 m, 灰白色中砂岩夹煤线, 因滑塌造成阶梯状同沉积小断层, 断距 2~15 mm; (d) 钻孔 ZKH1-1, 236.73 m, 灰色含砾粗砂岩, 发育正—反粒序; (e) 钻孔 ZKH1-1, 341.74 m, 灰白色粗砂岩夹煤线, 发育波状交错层理; (f) 钻孔 ZKH4-2, 368.03 m, 深灰色粉砂岩发育水平层理; (g) 钻孔 ZKH2-1, 319.60 m, 灰色粉砂岩发育爬升沙纹层理; (h) 钻孔 ZKH4-2, 134.09 m, 灰黑色泥岩, 质纯性脆; (i) 钻孔 ZKH2-1, 304.61 m, 灰黑色泥岩发育虫孔

(a) The Well ZKH1-2, 241.29 m, catastrophic contact between grayish white conglomerate and lacustrine mudstone with scour surface; (b) the Well ZKH4-2, 189.83 m, grayish white gravel-bearing coarse sandstone with of trough-shaped cross bedding; (c) the Well ZKH1-1, 296.35 m, the grayish white sandstone coal-intercalation line has small step-like synsedimentary faults with a fault spacing of 2~15 mm due to the collapse; (d) the Well ZKH1-1, 236.73 m, gray gravel-bearing coarse sandstone with positive—negative grain sequence; (e) the Well ZKH1-1, 341.74 m, greyish white coarse sandstone coal line with wavy cross bedding; (f) the Well ZKH4-2, 368.03 m, horizontal bedding of dark grey siltstone; (g) the Well ZKH2-1, 319.60 m, grey siltstone develops creeping sandy bedding; (h) the Well ZKH4-2, 134.09 m, grey—black mudstone, pure and brittle; (i) the Well ZKH2-1, 304.61 m, insect hole development in grey—black mudstone

于各井所处的亚环境不同, 沉积序列上也存在差异(图13)。例如钻孔 ZKH1-1 上部砂岩段主要为扇三角洲平原亚相沉积, 表现为厚层粗碎屑沉积物沉积, 泥岩则以洪泛沉积物形式存在, 由于靠近物源,

水动力表现为近源强流, 沉积物受重力流影响快速卸载, 扇三角洲快速建造, 并暂时处于弱氧化—弱还原环境, 总体表现为加积序列。下部的扇三角洲前缘亚相砂体, 由于受到牵引流和重力流的双重影响,

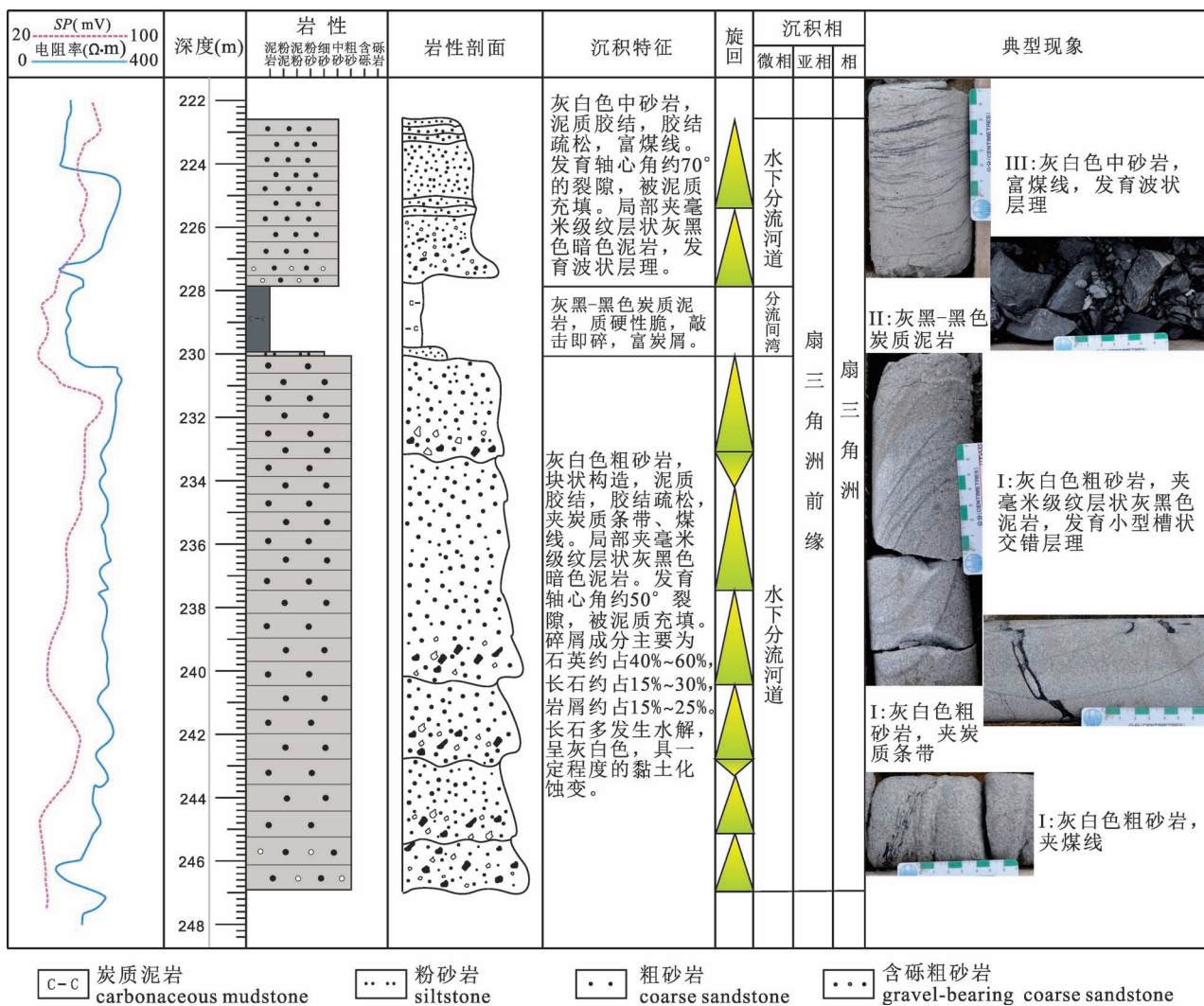


图 10 三江盆地鹤岗凹陷共青农场钻孔 ZKH1-1 猴石沟组 222.61~264.70 m 段扇三角洲前缘沉积序列

Fig. 10 The front fan delta depositional sequence of the Houshigou Formation from 222.61~264.70 m of the Well ZKH1-1 in Gongqing Farm, the Hegang Depression, Sanjiang Basin

发育典型的滑塌构造,又加上波浪簸选作用,垂向上可见明显正—反粒序组合,冲刷面频繁出现,具河道滞留沉积特征,常形成丰富的层理构造。钻孔ZKH2-1的下部砂体主要为滨浅湖沉积,表现为砂泥互层。综合而言,前缘亚相的河道砂体与浅湖泥可形成良好的“泥—砂—泥”结构。

3.3 沉积相展布特征

图14为1条近北东—南西方向展布的连井剖面,总体上,北粗南细,由于水体较浅,碎屑沉积物分布于水上和水下,形成了一套近源、分选中等—较差的粗碎屑沉积,即扇三角洲沉积。靠近北部物源区发育扇三角洲平原辫状河道粗碎屑沉积夹薄层河道间的细粒沉积,其砂砾岩复合体厚度较大,由于沉积物源供给充分,沉积物较粗,河道宽度大,表现为多

期砾质河道沉积叠置而成,自下而上为多个由粗至细的正韵律旋回组成,单次河道充填厚度一般为2~58 m,砂地比一般在0.4以上。侧向迁移强,河道内砂体相互切割改造,早期河道上部细粒沉积多被晚期河道改造移除,因此,形成了厚度大、泥岩夹层少的砂砾岩层。向湖盆中心方向逐渐过渡为扇三角洲前缘亚相,沉积范围明显扩大,发育多支水下分流河道,物质供应较辫状河道弱,粒度相对较细,此时研究区沉积的含砾砂岩都经过了一定距离的搬运,泥质含量较低,分选中—好,单次河道充填厚度一般2~26 m,砂地比一般在0.25~0.40。

在2条野外地质露头和8口铀矿地质钻孔的岩芯观察描述、测井相分析等资料综合分析基础上,编制了猴石沟组沉积相平面图(图15),结果表明,整

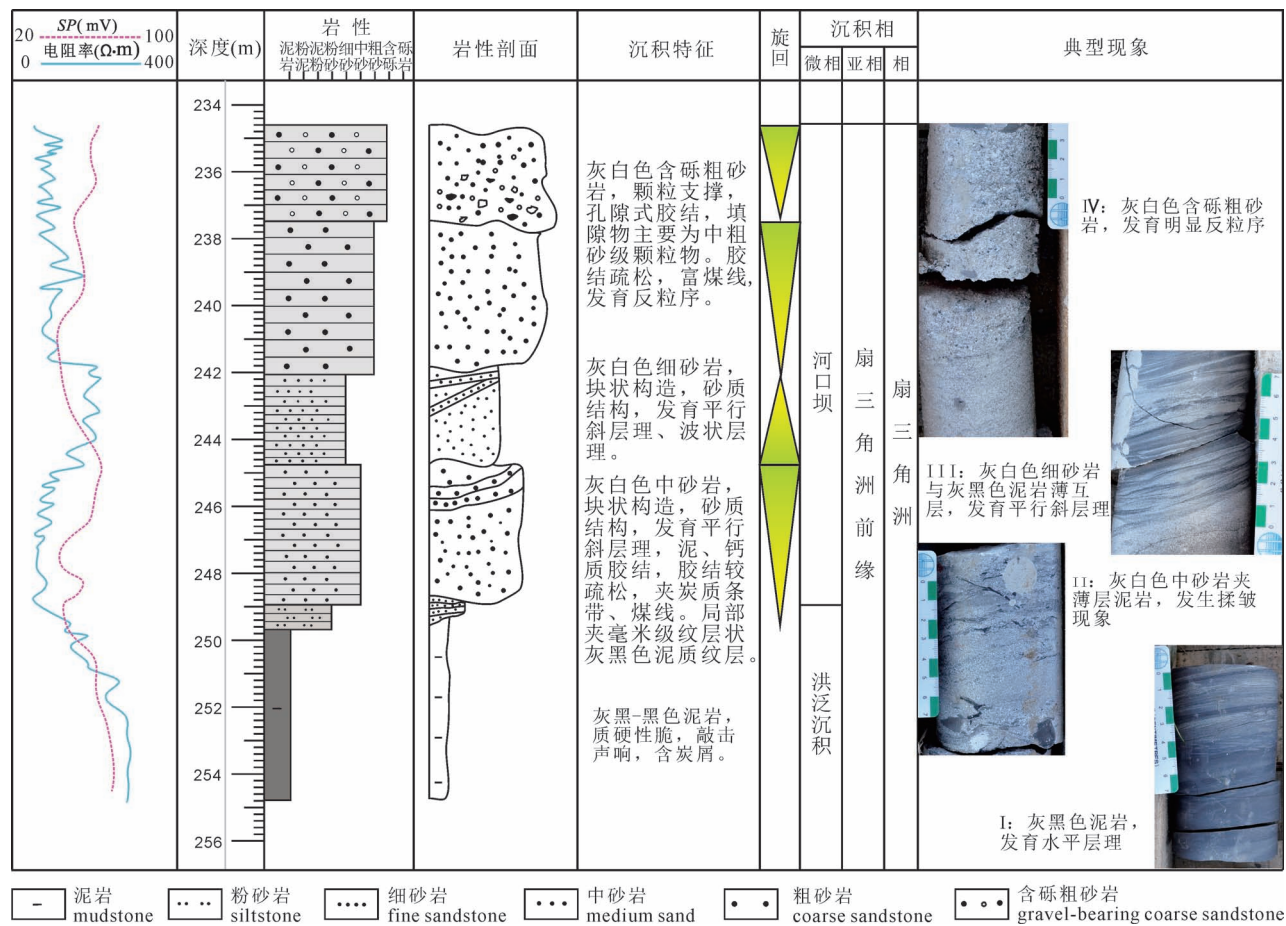


图 11 三江盆地鹤岗凹陷金山村钻孔 ZKH1-2 猴石沟组 235. 54~254. 79 m 段扇三角洲前缘河口坝沉积序列

Fig. 11 The front fan delta mouth-bar depositional sequence of the Houshigou Formation from 235. 54~254. 79 m of the Well ZKH1-2 in Jinshan village, the Hegang Depression, Sanjiang Basin

个研究区为一套扇三角洲入湖的粗碎屑沉积体系, 沉积中心位于宝泉岭一带, 发育滨浅湖相沉积。自北而南发育扇三角洲平原和前缘亚相, 沉积过程中伴随较强的波浪改造作用, 导致扇三角洲平原的分布范围有限, 形成“大前缘小平原”的沉积特征。平

原亚相发育辫状河道, 岩性主要由砂砾岩、含砾粗砂岩和粗砂岩组成, 砾石砾径变化范围大, 反映水动力能量多变, 受到了重力流的更大影响。前缘亚相发育水下分流河道, 砂体连续性较好, 河道延伸较远, 砾径变化较辫状河道范围小, 兼具反正旋回, 既有水

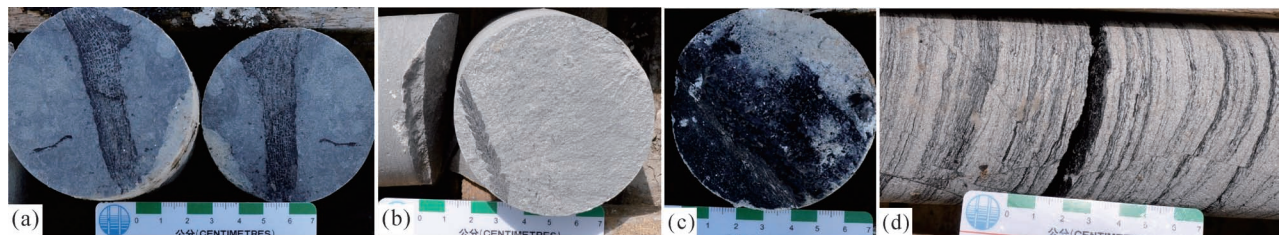


图 12 三江盆地鹤岗凹陷猴石沟组典型岩芯特征

Fig. 12 Typical cores characteristics of the Houshigou Formation in the Hegang Depression, Sanjiang Basin

- (a) The ZKH1-2, 164.37 m, 灰黑色泥岩含炭化植物茎秆化石;
- (b) the ZKH1-1, 328.27 m, 深灰色粉砂岩含保存完整的炭化植物叶片;
- (c) the ZKH1-1, 290.06 m, 灰白色含砾细砂岩夹煤线, 断切面;
- (d) the ZKH1-1, 375.39 m, 灰白色粗砂岩富煤线

(a) The ZKH1-2, 164.37 m, carboniferous plant stalk fossils from gray-black mudstone; (b) the ZKH1-1, 328.27 m, dark grey siltstone contains well-preserved leaves of carbonized plants; (c) the ZKH1-1, 290.06 m, grayish white gravel-bearing fine sandstone intercalation line, broken section; (d) the ZKH1-1, 375.39 m, grey-white coal-rich coal line of coarse sandstone

亚相	微相类型垂向组合		主要特征	水动力解释	进积/退积	成因解释模式	典型图片	代表井
	组合类型	模式						
扇三角洲平原相	重力流水道+洪泛沉	 A vertical column showing a thick grey band at the top representing a gravity flow channel, followed by a thin white band, and then a thin grey band at the bottom representing alluviation.	块状砾岩 冲刷面 块状泥岩	泥石流 冲刷 静水+漫溢	 A vertical color bar with a gradient from yellow at the top to green at the bottom, with a red dot indicating the transition point.	 A diagram showing a cross-section of a channel with a red dot at the base, followed by a dashed line representing a backfilling process.	 A photograph of a rock sample with a ruler for scale.	ZKH1-1
	漫溢+静水	 A vertical column showing a thin grey band at the top representing overflow, followed by a thin white band, and then a thin grey band at the bottom representing still water.	含斑点状 微砂砾 冲刷面 块状泥岩	漫溢 微冲刷 静水	 A vertical color bar with a gradient from yellow at the top to green at the bottom, with a red dot indicating the transition point.	 A diagram showing a cross-section of a channel with a red dot at the base, followed by a dashed line representing a backfilling process.	 A photograph of a rock sample with a ruler for scale.	ZKH4-2
扇三角洲前缘亚	滑动+滑塌	 A vertical column showing a thick grey band at the top representing sliding, followed by a thin white band, and then a thin grey band at the bottom representing landslides.	包卷 颗粒定向 剪切面 滑塌面	重力-水湿 润滑-诱发 因素	 A vertical color bar with a gradient from yellow at the top to green at the bottom, with a red dot indicating the transition point.	 A diagram showing a cross-section of a channel with a red dot at the base, followed by a dashed line representing a backfilling process.	 A photograph of a rock sample with a ruler for scale.	ZKH1-1
	下湖重力坝流水道	 A vertical column showing a thick grey band at the top representing a gravity dam in a lake, followed by a thin white band, and then a thin grey band at the bottom representing a waterway.	 A wavy line pattern representing wave action.	波浪簸选 冲刷	 A vertical color bar with a gradient from yellow at the top to green at the bottom, with a red dot indicating the transition point.	 A diagram showing a cross-section of a channel with a red dot at the base, followed by a dashed line representing a backfilling process.	 A photograph of a rock sample with a ruler for scale.	ZKH1-2
	扇浅湖砂坝砂滩	 A vertical column showing a thick grey band at the top representing a sandbar in a shallow lake, followed by a thin white band, and then a thin grey band at the bottom representing a sandbar.	 A wavy line pattern representing wave action.	波浪簸选+近源 波浪簸选+远源	 A vertical color bar with a gradient from yellow at the top to green at the bottom, with a red dot indicating the transition point.	 A diagram showing a cross-section of a channel with a red dot at the base, followed by a dashed line representing a backfilling process.	 A photograph of a rock sample with a ruler for scale.	ZKH1-3
滨浅湖	滨湖砂泥滩	 A vertical column showing a thick grey band at the top representing a lake margin sandbar, followed by a thin white band, and then a thin grey band at the bottom representing a sandbar.	 A wavy line pattern representing wave action.	波浪簸选 静水 波浪簸选 静水	 A vertical color bar with a gradient from yellow at the top to green at the bottom, with a red dot indicating the transition point.	 A diagram showing a cross-section of a channel with a red dot at the base, followed by a dashed line representing a backfilling process.	 A photograph of a rock sample with a ruler for scale.	ZKH2-1

图 13 三江盆地鹤岗凹陷猴石沟组沉积微相组合和演化综合分析图

Fig. 13 Comprehensive analysis map of the sedimentary microfacies assemblage and evolution of the Houshigou Formation in the Hegang Depression, Sanjiang Basin

道也有扇体,代表了河流的牵引流作用,说明了滨浅海环境的波浪水动力和碎屑供应互动的结果。

3.4 沉积相模式

根据平、剖面沉积微相特征,总结了该研究区的扇三角洲沉积模式(图 16),受构造和气候影响,沉积相带大致呈北东—南西向展布。湖泊逐渐扩张,沉积体系由盆中向盆地边缘逐渐退积,物源主要来自北部和西部山区,沉积物供给充分,粒度粗,砂地比含量高,反映了近物源的沉积特征。来自北部和西部山区的碎屑物质经过搬运,形成了浅水的扇三角洲、滨浅湖沉积,水动力较强,砂体规模大,砂地比高,粒度粗,为近源充分供屑沉积特征。同时沉积过程伴随较强的波浪改造作用,导致扇三角洲平原的分布范围有限,形成“大前缘小平原”的沉积特征。

陆上部分为扇三角洲平原,岩性以辫状河道形成的厚层砂砾岩、含砾粗砂岩为主,进入水体后向前推进形成扇三角洲前缘沉积,岩性以水下分流河道成因的灰—灰白色局部含砾的中粗砂岩为主。宝泉岭农场一带发育半深湖相沉积,沉积物粒度最细,以泥岩、粉砂质泥岩为主,是猴石沟组的沉积中心。

4 砂体类型与找矿方向

4.1 砂体类型与找矿类型

砂岩型铀矿的形成需要好的储集空间—砂体,而沉积相和微相对砂岩型铀矿矿化的控制明显(于文卿等,2000;王争鸣,2003;郭庆银等,2006;陈超等,2016;何中波等,2018b;聂逢君等,2018)。猴石沟组较有利的成矿砂体类型主要有两类(表 1):扇

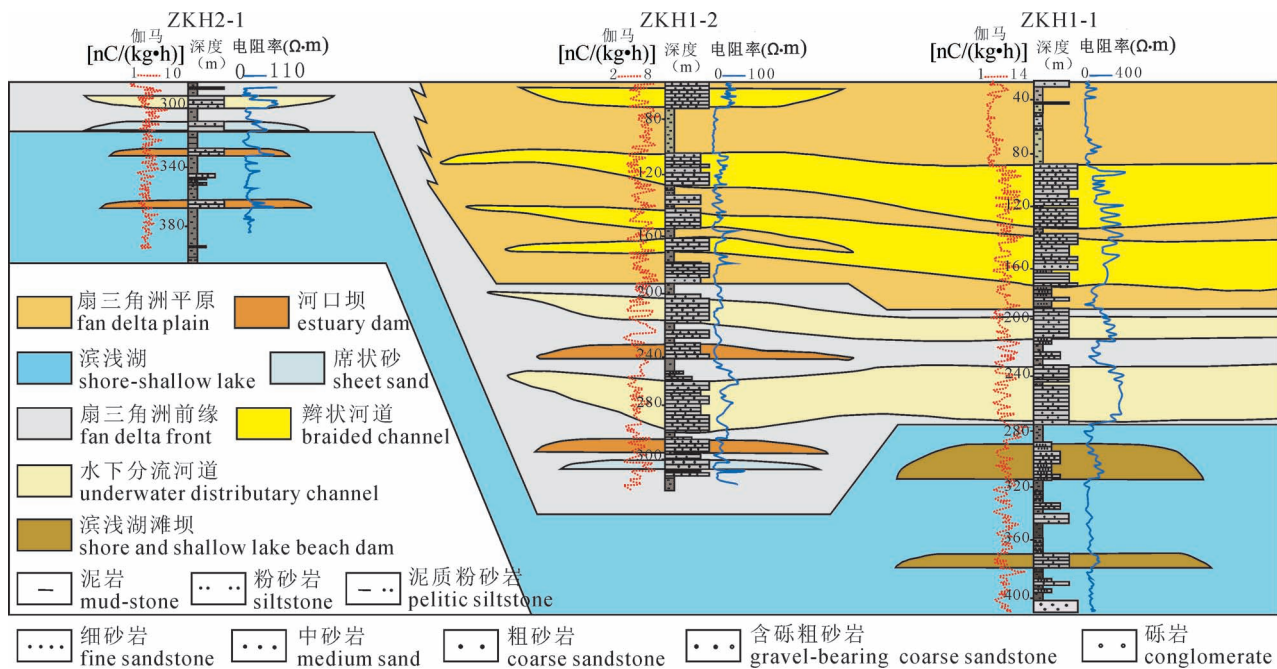


图 14 三江盆地鹤岗凹陷猴石沟组南北向沉积相剖面图(剖面位置见图 15)

Fig. 14 The north—south sedimentary facies profile of the Houshigou Formation in the Hegang Depression, Sanjiang Basin (profile location see fig. 15)

三角洲平原辫状河微相中发育的辫状河道砂体和扇三角洲前缘分流河道微相中发育的水下分流河道砂体。

辫状河道砂体沉积物粒度偏粗, 主要为河道砾岩、砂砾岩、砂岩等, 砂体发育厚度大(2~58 m), 岩性以中—粗粒长石岩屑砂岩和岩屑砂岩为主, 成熟度较低, 孔渗性较好, 砂体垂向和横向延伸均较广, 具有较好的连通性, 富含有机质及碳屑, 可为富铀流体的运移和铀元素的富集提供良好的空间及还原容量。横向常与沼泽沉积呈超覆或舌状交错接触, 又由于靠近物源, 易发育沉积间断面并缺乏泥岩沉积的隔水层, 垂向上有利于潜水氧化带的发育。

水下分流河道砂体, 主要由一套灰色粗碎屑岩

组成, 成熟度相对较高, 物性好, 有利于后期含铀含氧流体在其中的运移推进, 砂岩中富含煤线和炭屑等还原物质, 局部夹薄煤层, 说明有机质含量高, 还原容量丰富, 有利于含铀—煤沉积建造的形成, 有利于铀物质在有机质、 H_2S 等还原剂的吸附还原作用下的富集, 与厚层的间湾泥或浅湖泥构成“泥—砂—泥”结构, 可作为寻找层间氧化带型砂岩型铀矿的主攻类型。

4.2 找矿方向

研究区主要为扇三角洲—湖泊沉积环境, 扇三角洲平原辫状河道和扇三角洲前缘分流河道是重要的找矿方向。

扇三角洲平原辫状河道主要发育于沿愚公村、

表 1 鹤岗凹陷猴石沟组砂体特征对比表

Table 1 Comparison of sand bodies features of the Houshigou Formation in the Hegang Depression

亚相	微相	主要特点	渗透性	空间展布	还原剂容量	岩性组合	铀成矿潜力
扇三角洲平原	辫状河道 河道间	块状, 厚度大, 成熟度低 薄层, 厚度变化大	好 差	稳定 不稳定	中—高 高	泥—砂—泥 泥、砂互层	好 差
扇三角洲前缘	水下分流河道 河口坝 席状砂 分流间湾	块状, 厚度大, 成熟度高 薄—中层, 累计厚, 分布局限 薄—中层, 分布局限 多泥, 炭屑	中 中—差 差 差	稳定 不稳定 稳定 不稳定	高 中 中 中	泥—砂—泥 砂岩夹泥岩 砂岩夹泥岩 泥岩	很好 差 差 差
滨浅湖	滩坝	厚层, 块状, 成熟度高	差	不稳定	高	泥砂互层	差

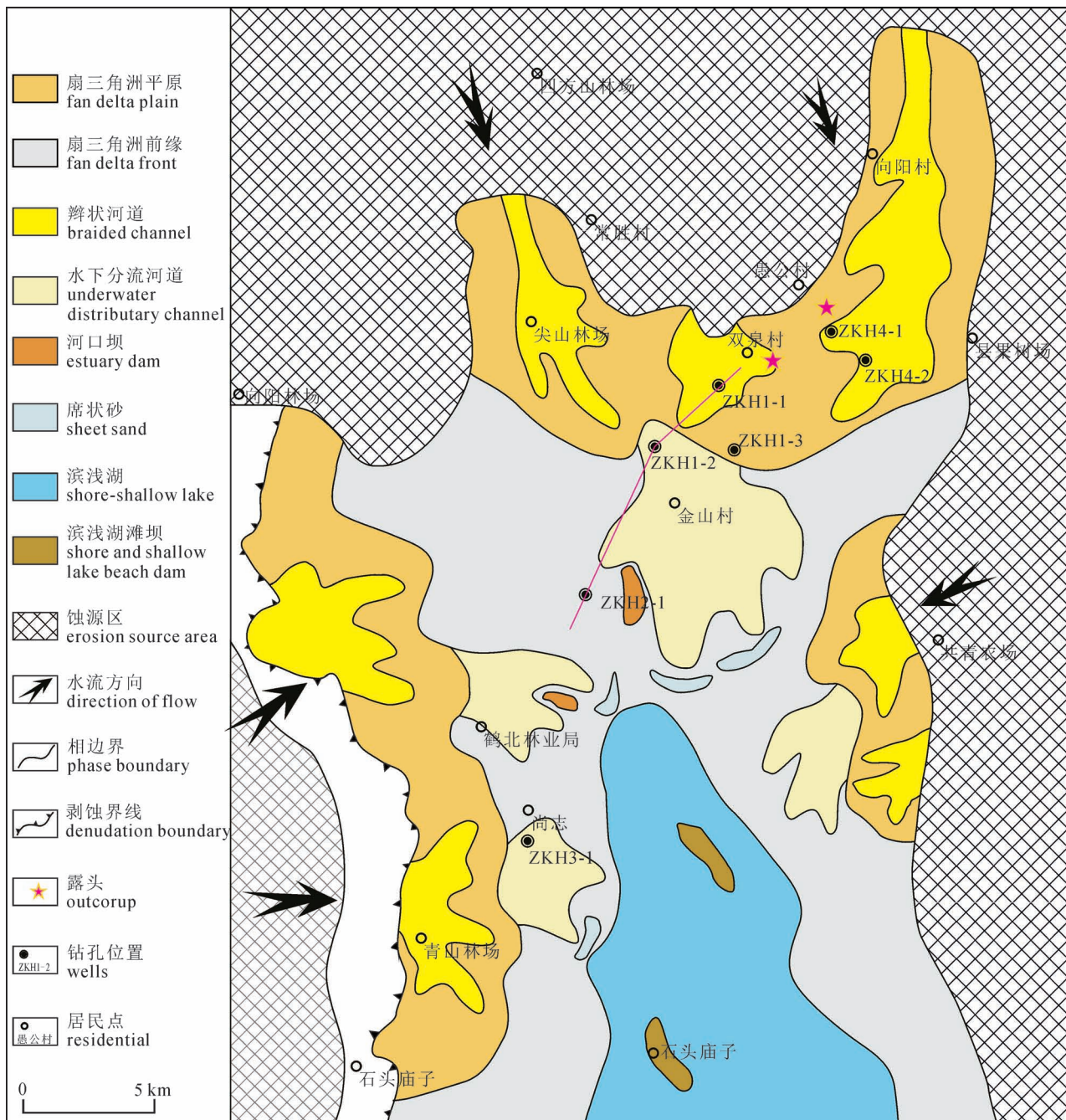


图 15 三江盆地鹤岗凹陷猴石沟组沉积相平面图

Fig. 15 Sedimentary facies plane diagram of the Houshigou Formation in the Hegang Depression, Sanjiang Basin

双泉村及平行于盆缘一带(距离盆缘 3~6 km), 适合作为砂岩型铀矿潜水氧化的有利勘探区域, 是目前勘探的主要有利区域; 扇三角洲前缘水下分流河道主要发育于金山村、鹤北林业局、尚志一带, 适合作为砂岩型铀矿层间氧化的重点勘探区域。

5 结论

通过对鹤岗凹陷猴石沟组沉积时期沉积体系和沉积相的系统研究, 得出以下几点认识:

(1) 猴石沟组砂岩以长石岩屑砂岩和岩屑砂岩为主; 通过微量元素 $V/(V+Ni)$ 值反映猴石沟组沉积时期为陆相淡水环境, 且不管是砂岩还是泥岩中,

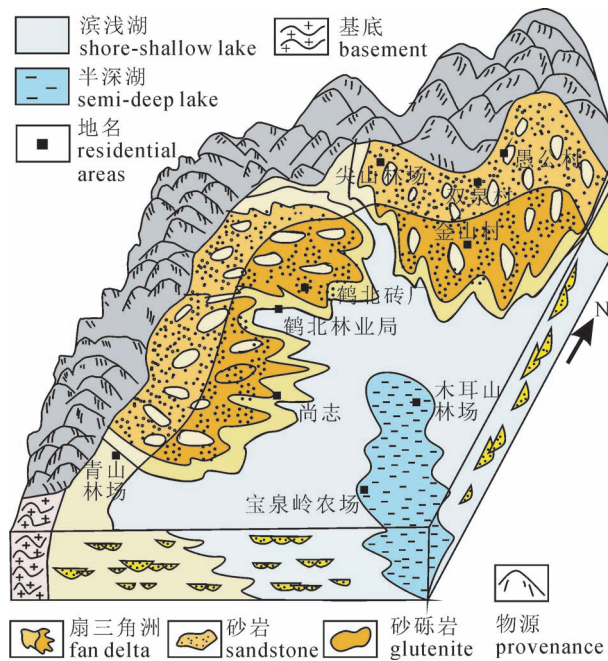


图 16 三江盆地鹤岗凹陷猴石沟组立体沉积模式图

Fig. 16 Sedimentary stereoscopic pattern diagram of the Houzhigou Formation in the Hegang Depression, Sanjiang Basin

炭屑和炭化植茎化石都异常丰富,反映了具较高的还原容量。

(2) 野外露头、岩芯、钻井、测井等资料综合研究表明,鹤岗凹陷猴石沟组广泛发育“近源、浅水”的扇三角洲沉积,并划分出扇三角洲平原和扇三角洲前缘2种亚相以及辫状河道、漫滩沼泽、水下分流河道、河口坝、席状砂和分流间湾6种微相。

(3) 研究区下白垩统猴石沟组(K_1h)沉积物表现为水动力强、砂体规模大、粒度粗的特点,为近源、充分供屑的沉积特征,还原容量高,是一套有利的含矿建造,辫状河道砂体可作为寻找潜水氧化型的重点类型,而水下分流河道砂体是作为寻找层间氧化型的主攻类型。

参 考 文 献 / References

(The literature whose publishing year followed by a “&” is in Chinese with English abstract; The literature whose publishing year followed by a “#” is in Chinese without English abstract)

蔡超,时伟,曹代勇. 2016. 鹤岗盆地断裂构造特征与地应力演化

史分析. 中国煤炭地质, 28(3): 8~25.

程三友,刘少峰,苏三. 2012. 黑龙江三江盆地绥滨坳陷构造特征

分析. 东华理工大学学报(自然科学版), 35(4): 322~328.

陈东旭. 2016. 黑龙江东部中—新生代构造演化与低温热年代学研

究. 导师:陈汉林. 杭州:浙江大学博士学位论文:1~187.

陈戴生,李胜祥,蔡煜琦. 2003. 我国中新生代盆地砂岩型铀矿研究现状及发展方向的探讨. 沉积学报, 21(1): 113~117.

蔡煜琦,张金带,李子颖,郭庆银,宋继叶,范洪海,刘武生,漆富成,张明林. 2015. 中国铀矿资源特征及成矿规律概要. 地质学报, 89(6): 1051~1069.

陈超,刘洪军,侯惠群,韩绍阳,柯丹,白云生,欧光习,李言瑞. 2016. 鄂尔多斯盆地北部直罗组黄铁矿与砂岩型铀矿化关系研究. 地质学报, 90(12): 3375~3380.

邓宏文,钱凯. 1993. 沉积地球化学与环境分析. 兰州:甘肃科学技术出版社: 95~104.

范玉海,屈红军,王辉,杨县超,冯杨伟. 2012. 微量元素分析在判别沉积介质环境中的应用—以鄂尔多斯盆地西部中区晚三叠世为例. 中国地质, 39(2): 382~389.

方石,张培震,刘招君,刘金平,田军. 2012. 东三江盆地南部白垩纪以来的沉积特征及其演化. 吉林大学学报(地球科学版), 42(1): 66~76.

郭庆银,李子颖,杨圣彬,杨圣彬,杨立志. 2006. 鄂尔多斯盆地西北部白垩系沉积特征. 铀矿地质, 5(3): 143~150.

何中波,刘章月,杨烨,郭强,宋继叶,冀华丽. 2016. 准噶尔盆地中新生代构造沉积演化与砂岩型铀成矿作用关系探讨. 新疆地质, 34(3): 410~417.

何中波,冀华丽,曹建辉,杨帆. 2018a. 黑龙江三江盆地中东部白垩纪以来沉积演化特征及铀矿化有利找矿层位. 世界核地质科学, 35(4): 187~202.

何中波,秦明宽,宋继叶,郭强,许强,刘章月,杨烨,黄少华. 2018b. 准噶尔盆地东北部侏罗系砂岩型铀成矿环境与找矿方向探讨. 矿床地质, 37(1): 175~190.

侯伟,刘招君. 2007. 黑龙江省东部绥滨坳陷下白垩统泥岩稀土元素地球化学特征. 古地理学报, 9(2): 207~215.

和钟铧,刘招君,陈秀艳,何玉平,陈永成. 2008. 黑龙江省东部残留盆地群早白垩世沉积相特征及演化. 古地理学报, 10(2): 151~158.

季汉成,门相勇,翁庆萍,杨东杰,孟培伟. 2013. 东北大三江地区早白垩世岩相古地理研究. 地球科学与环境学报, 35(2): 81~91.

贾承造,郑民. 2010. 东北白垩纪大三江盆地沉积构造演化及其残留盆地群的油气勘探意义. 大庆石油学院学报, 34(6): 1~12.

李纯杰,司黎,王志林. 2010. 鹤岗煤田深部煤炭资源潜力分析研究. 中国煤炭地质, 22(5): 18~22.

李子颖,秦明宽,蔡煜琦,范洪海,程纪星,郭冬发,叶发旺,陆士立,梁春利. 2015. 铀矿地质基础研究和勘查技术研发重大进展与创新. 铀矿地质, 31(1): 141~155.

刘孟骐,郭巍,于松,张海东,张丛. 2017. 三江盆地下白垩统穆棱组页岩气成藏地质条件研究. 世界地质, 36(1): 209~216.

梁奉奎,马立军,王文化,阎伟. 2001. 鹤岗煤田煤层气赋存规律. 煤炭技术, 20(4): 55~56.

廖群山,徐会建,杨建国,刘中良,穆献中. 2011. 大庆油田及其外围盆地非常规天然气资源勘探潜力. 天然气工业, 31(3): 26~30.

聂逢君,张成勇,姜美珠,严兆彬,张鑫,张进,乔海明,周伟. 2018. 吐哈盆地西南缘地区砂岩型铀矿含矿目的层沉积相与铀矿化. 古地理学报, 10(10): 3584~3602.

秦明宽,何中波,刘章月,郭强,宋继叶,许强. 2017. 准噶尔盆地砂岩型铀矿成矿环境与找矿方向研究. 地质论评, 63(5): 1255~1269.

陶树,汤达祯,周传伟,李凤,李婧婧,陈晓智,孟昌衷. 2009. 川东南—黔中及其周边地区下组合烃源岩元素地球化学特征及沉积环境意义. 中国地质, 36(2): 397~403.

- 温泉波, 刘永江, 韩国卿, 孙晓猛, 赵英利, 李伟. 2008. 黑龙江东部盆地群中、新生代构造演化. *世界地质*, 27(4): 370~377.
- 吴崇筠. 1986. 湖泊砂体类型. *沉积学报*, 4(4): 1~27.
- 王争鸣. 2003. 缺氧沉积环境的地球化学标志. *甘肃地质学报*, 12(2): 55~58.
- 许仔明, 许宏节, 胡志方, 袁桂林, 刘明慧. 2010. 三江盆地缓滨坳陷下白垩统煤系烃源岩评价. *成都理工大学学报(自然科学版)*, 37(1): 15~20.
- 熊国庆, 王剑, 胡仁发. 2008. 贵州梵净山地区震旦系微量元素特征及沉积环境. *地球学报*, 29(1): 51~60.
- 于文卿, 于恩君, 王统高, 屈旭钩. 2000. 砂体与可地浸砂岩型铀矿. *铀矿地质*, 16(5): 280~290.
- 杨子荣, 姜虹剑. 1997. 鹤岗盆地晚侏罗世石头河子组沉积环境及幕式聚煤作用. *沉积学报*, 15(3): 56~61.
- 张兴洲, 郭治, 曹振, 付秋林, 蒲建彬. 2015. 东北地区中—新生代盆地群形成演化的动力学背景. *地学前缘*, 22(3): 88~98.
- 张金带, 徐高中, 林锦荣. 2010. 中国北方6种新的砂岩型铀矿对铀资源潜力的提示. *中国地质*, 37(5): 470~477.
- 曾允孚, 夏文杰. 1986. 沉积岩石学. 北京: 地质出版社, 87~98.
- 张君峰, 许浩, 赵俊龙, 任鹏飞. 2018. 中国东北地区油气地质特征与勘探潜力展望. *中国地质*, 45(2): 260~273.
- 张天福, 孙立新, 张云, 程银行, 李艳锋, 马海林, 鲁超, 杨才, 郭根万. 2016. 鄂尔多斯盆地北缘侏罗纪延安组、直罗组泥岩微量元素、稀土元素地球化学特征及其古沉积环境意义. *地质学报*, 90(12): 3454~3472.
- 张云鹏, 任建业, 王姗, 赵学钦. 2016. 东北大三江盆地群早白垩世存在统一湖盆的沉积学证据. *中国地质*, 43(4): 1280~1290.
- 中国石油学会石油地质委员会. 1988. 碎屑岩沉积相研究. 北京: 石油工业出版社, 162~181.
- Algeo T J, Maynard J B. 2004. Trace-element behavior and redox facies in core shales of Upper Pennsylvanian Kansas-type cyclothems. *Chemical Geology*, 206: 289~318.
- Bhatia Mr. 1983. Plate tectonics and geochemical composition of sandstones. *Journal of Geology*, 91(6): 611~627.
- Bhatia Mr, Crook K A W. 1986. Trace element characteristics of graywackes and tectonic setting discrimination of sedimentary basins. *Contributions to Mineralogy and Petrology*, 92(2): 181~193.
- Cai Chao, Shi Wei, Cao Daiyong. 2016&. Faulted structural features and crustal stress evolution history analysis in Hegang Basin. *Coal Geology of China*, 28(3): 8~25.
- Cheng Sanyou, Liu Shaofeng, Su San. 2012&. Structure characteristics of Suibin sag in Sanjiang basin. *Journal of East China Institute of Technology*, 35(4): 322~328.
- Chen Dongxu. 2016. Mesozoic—Cenozoic tectonic evolution and low temperature thermochronological study of Eastern Heilongjiang, NE China. Zhejiang University. Professor: Chen Hanlin. Hangzhou: Zhejiang University, 1~187.
- Chen Daisheng, Li Shengxiang, Cai Yuqi. 2003. A discussion on research situation and development direction of sandstone-type uranium deposits in the Meso—Cenozoic basin of China. *Acta Sedimentologica Sinica*, 21(1): 113~117.
- Cai Yuqi, Zhang Jindai, Li Ziying, Guo Qingyin, Song Jiye, Fan Honghai, Liu Wusheng, Qi Fucheng, Zhang Minglin. 2015&. Outline of uranium resources characteristics and metallogenetic regularity in China. *Acta Geologica Sinica*, 89(6): 1051~1069.
- Chen Chao, Liu Hongjun, Hou Huiqun, Han Shaoyang, Ke Dan, Bai Yunsheng, Ou Guangxi, Li Yanrui. 2016&. The relationship between pyrite and sandstone-hosted uranium mineralization of the Zhiluo Formation in the northern Ordos Basin. *Acta Geologica Sinica*, 90(12): 3375~3380.
- Deng Hongwen, Qian Kai. 1993#. *Sedimentary Geochemistry and Environment Analysis*. Lanzhou: Gansu Science and Technology Press, 95~104.
- Fan Yuhai, Qu Hongjun, Wang Hui, Yang Xianhui, Feng Yangwei. 2012. The application of trace elements analysis to identifying sedimentary media environment; a case study of Late Triassic strata in the middle part of western Ordos Basin. *Geology in China*, 39(2): 382~389.
- Fang Shi, Zhang Peizhen, Liu Zhaojun, Liu Jinping, Tian Jun. 2012&. Sedimentation features and its evolution since Cretaceous in the south of Eastern Sanjiang Basin. *Journal of Jilin University (Earth Science Edition)*, 42(1): 66~76.
- Guo Qingyin, Li Ziying, Yang Shengbin, Yang Shengbin, Yang Lizhi. 2006&. Sedimentary characteristics of Cretaceous in northwestern Ordos Basin. *Uranium Geology*, 5(3): 143~150.
- Hatch J R, Leventhal J S. 1992. Relationship between inferred redox potential of the depositional environment and geochemistry of the Upper Pennsylvanian (Missourian) Stark Shale Member of the Dennis limestone, Wabaunsee County, Kansas, USA. *Chemical Geology*, 99(1): 65~82.
- He Zhongbo, Ji Huali, Cao Jianhui, Yang Fan. 2018&. Sedimentary evolution characteristics since Cretaceous and favourable horizons of sandstone-hosted uranium mineralization in middle-east Sanjiang basin, Heilongjiang. *World Nuclear Geoscience*, 35(4): 187~202.
- He Zhongbo, Qin Mingkuan, Song Jiye, Guo Qiang, Xu Qiang, Liu Zhangyue, Yang Ye, Huang Shaohua. 2018&. A Study of metallogenic environments and prospecting direction of Jurassic sandstone-type uranium deposit in northeastern Junggar Basin. *Mineral Deposits*, 37(1): 175~190.
- Hou Wei, Liu Zhaojun. 2007&. REE geochemical characteristics of the Lower Cretaceous mudstone in Suibin Depression of eastern Heilongjiang Province. *Journal of Palaeogeography*, 9(2): 207~215.
- He Zhongbo, Liu Zhangyue, Yang Ye, Guo Qiang, Song Jiye, Ji Huali. 2016&. Mesozoic Cenozoic tectonic—sedimentary evolution and Metallogenesis of sandstone-type uranium deposit in Junggar Basin. *Xijiang Geology*, 34(3): 410~417.
- He Zhonghua, Liu Zhaojun, Chen Xiuyan, He Yuping, Chen Yongcheng. 2008&. Sedimentary facies characteristics and their evolution of the Early Cretaceous relict basins in eastern Heilongjiang Province. *Journal of Palaeogeography*, 10(2): 151~158.
- Ji Hancheng, Men Xiangyong, Wong Qingping, Yang Dongjie, Meng Peiwei. 2013&. Study on Early Cretaceous lithofacies paleogeograph in paleogeography in Dasanjiang area of Northeast China. *Journal of Earth Sciences and Environment*, 35(2): 81~91.
- Jia Chengzao, Zheng Min. 2010&. Sedimentary history, tectonic evolution of Cretaceous Dasanjiang Basin in Northeast China and the significance of oil and gas exploration of its residual basins. *Journal of Daqing Petroleum Institute*, 34(6): 1~12.
- Lerman A, Baccini P. 1978. Lakes—chemistry, geology, physics. *Journal of Geology*, 88(2): 249~250.
- Li Chunjie, Si Li, Wang Zhilin. 2010&. Hegang coalfield deep part coal resource potential analytic investigation. *Coal Geology of China*, 22(5): 18~22.
- Li Ziying, Qin Mingkuan, Cai Yuqi, Fan Honghai, Cheng Jixing, Guo Dongfa, Ye Fawang, Lu Lishi, Liang Chunli. 2015&. Great progress and breakthrough of China's uranium exploration in new

- century. *Uranium Geology*, 31(1): 141~155.
- Liu Mengqi, Guo Wei, Yu Song, Zhang Haidong, Zhang Cong. 2017&. Geological conditions of shale gas reservoirs of Lower Cretaceous Muling Formation in Sanjiang Basin. *Global Geology*, 36(1): 209~216.
- Liang Fengkui, Ma Lijun, Wang Weihua, Yan Wei. 2001&. Rules of the storage of coal seam gas in Hegang coal field. *Coal Technology*, 20(4): 55~56.
- Liao Qunshan, Xu Huijian, Yang Jianguo, Liu Zhongliang, Mu Xianzhong. 2011&. Unconventional natural gas potentials of the Daqing Oil Field and its peripheral basins. *Natural Gas Industry*, 31(3): 26~30.
- Nie Fengjun, Zhang Chengyong, Jiang Meizhu, Yan Zhaobin, Zhang Xin, Zhang Jin, Qiao Haiming, Zhou Wei. 2018&. Relationship of depositional facies and microfacies to uranium mineralization in sandstone along the southern margin of Turpan—Hami Basin. *Earth Science*, 10(10): 3584~3602.
- Qin Mingkuan, Huang Shaohua, He Zhongbo, Xu Qiang, Song Jiye, Liu Zhangyue, Guo Qiang. 2018. Evolution of tectonic uplift, hydrocarbon migration, and uranium mineralization in the NW Junggar Basin: an apatite fission-track thermochronology study. *Acta Geologica Sinica (English Edition)*, 92(5): 1901~1916.
- Qin Mingkuan, He Zhongbo, Liu Zhangyue, Guo Qiang, Song Jiye, Xu Qiang. 2017&. Study on metallogenic environments and prospective direction of sandstone type uranium deposits in Junggar Basin. *Geological Review*, 63(5): 1255~1269.
- Ribouleau A, Baudin F, Deconinck J F, Derenne S, Largeau C, Tribouillard N. 2003. Depositional conditions and organomatter preservation pathways in an epicontinental environment: the Upper Jurassic Kashpir oil shales (Volga Basin, Russia). *Palaeogeogr. Palaeoclimatol. Palaeoecol.*, 197: 171~197.
- Rimmer S M, Thompson J A, Goodnight S A, Robl T L. 2004. Multiple controls on the preservation of organic matter in Devonian ~ Mississippian marine black shales: geochemical and petrographic evidence. *Palaeogeogr. Palaeoclimatol. Palaeoecol.*, 215: 125~154.
- Scheffler K, Buehmann D, Schwark L. 2006. Analysis of late Palaeozoic glacial to postglacial sedimentary successions in South Africa by geochemical proxies—Response to climate evolution and sedimentary environment. *Palaeo*, 240(6): 184~203.
- Tribouillard N, Algeo T J, Lyons T, Ribouleau A. 2006. Trace metals as paleoredox and paleoproduction proxies: An update. *Chem. Geol.*, 232: 12~32.
- Wen Quanbo, Liu Yongjiang, Cao Zhen, Sui Xiaomeng, Zhao Yingli, Li Wei. 2008&. Mesozoic and Cenozoic tecnoic evolution of the basin group in eastern Heilongjiang, China. *Global Geolgy*, 27(4): 370~377.
- Wu Chongjun. 1986. Sand bodies in lake basin. *Acta Sedimentologica Sinica*, 4(4): 1~27.
- Wang Zhengming. 2003&. Geochemical indicators for diagnosing anoxic sedimentary environment. *Acta Geologica Gansu*, 12(2): 55~58.
- Xu Ziming, Xu Hongjie, Hu Zhifang, Yuan Guolin, Liu Minghui. 2010&. Evaluation of the source rocks from the Lower Cretaceous coal measure strata in the Suibin depression of Sanjiang basin, China. *Journal Of Cheng Du University of Technology (Science & Technology Edition)*, 37(1): 15~20.
- Xiong Guoqing, Wang Jian, Hu Renfa. 2008&. Trace element characteristics and sedimentary environment of the simian system of province. *Acta Geoscientifica Sinica*, 29(1): 51~60.
- Yu Wenqing, Yu Enjun, Wang Tonggao, Qu Xugao. 2000&. Sand body and in-situ leachable sandstone-type uranium deposit. *Uranium Geology*, 16(5): 180~190.
- Yang Zirong, Jiang Hongjian. 1997&. Depositional environments of the Shitouhezi Formation and its characteristics of the episodic coal accumulation, Upper Jurassic Hegang Basin, Heilongjiang Province. *Acta Sedimentologica Sinica*, 15(3): 56~61.
- Zeng Yunfu, Xia Weijie. 1986#. *Sedimentary Petrology*. Beijing: Geological Publishing House; 87~98.
- Zhang Xingzhou, Guo Ye, Cao Zhen, Fu Qiulin, Pu Jianbin. 2015&. Dynamic evolution of the Mesozoic—Cenozoic basins in the northeastern China. *Earth Science Frontiers*, 22(3): 88~98.
- Zhang Jindai, Xu Gaozhong, Lin Jinrong. 2010&. The implication of six kinds of new sandstone-type uranium deposits to uranium resources potential in North China. *Geology in China*, 37(5): 470~477.
- Zhang Junfeng, Xu Hao, Zhao Junlong, Ren Pengfei. 2018&. Geological characteristics and exploration potential of oil and gas in the northeast area of China. *Geolgy in China*, 45(2): 260~273.
- Zhang Tianfu, Sun Lixin, Zhang Yun, Cheng Yinhang, Li Yanfeng, Ma Hailin, Lu Chao, Yang Cai, Guo Genwan. 2016&. Geochemical characteristics of the Juiaassic Yan'an and Zhiluo Formations in the northern margin of Ordos Basin and their paleoenvironmental implications. *Acta Geologica Sinica*, 90(12): 3454~3472.
- Zhang Yunpeng, Ren Jianye, Wang Shan, Zhao Xueqin. 2016&. The sedimentary evidence for the exitence of unified basin in Early Cretaceous in Dasanjiang basin group , Northeast China. *Geology in China*, 43(4): 1280~1290.
- Petroleum Geology Institute of Chinese Petroleum Society. 1988. *Study of Clastic Sedimentary Facies*. Beijing: Petroleum Industry Press; 162~181.

Sedimentary characteristics of Lower Cretaceous Houshigou Formation in Hegang Depression, Sanjiang Basin, Heilongjiang Province

JI Huali¹⁾, HE Zhongbo¹⁾, QIN Mingkuan¹⁾, WEI Sanyuan¹⁾, CAO Jianhui¹⁾, YANG Fan²⁾

1) Beijing Research Institute of Uranium Geology, Beijing, 100029;

2) Sinopec Research Institute of Petroleum Engineering, Beijing, 100101

Objectives: The sedimentary facies types of the favorable ore-forming sand bodies of the Houshigou Formation are preliminarily discussed under the guidance of the metallogenic theory of sandstone-type uranium deposits, combined with a small amount of sample analysis and thin section identification work, through the comprehensive

utilization of outcrop and borehole data in the north of Hegang Depression.

Methods: In this paper, the main petrological characteristics, sedimentary facies types and distribution characteristics of the Lower Cretaceous Houshigou Formation in the study area are comprehensively studied.

Conclusions: It is shown that: ①The sand bodies of the Houshigou Formation are mainly feldspathic lithic sandstones and lithic sandstones, which are mainly continental freshwater sedimentary environments with high reduction capacity; ②The Houshigou Formation in the study area is mainly fan delta sedimentary environment, and is divided into six microfacies: braided channel, floodplain swamp, underwater distributary channel, estuary bar, sheet sand and distributary bay; ③The submerged braided channel sand body of the Houshigou Formation can be used as a key type for searching for phreatic-oxidized-type sandstoneuranium deposit, while the underwater distributary channel sand body is the main type for searching for interlayer-oxidized-zone-type sandstone uranium deposit.

Keywords: Lower Cretaceous Houshigou Formation; fan delta; sedimentary facies; Hegang Depression, Sanjiang Basin, Heilongjiang Province

Acknowledgements: This study is financially supported by National Defense Pre-research Foundation of China and uranium prospecting project of China Nuclear Geology(Nos. 201713, 201929). The authors would like to thank prof. Cai Yuqi of Institute of Geology and Mineral Resource for the constructive and thorough reviews.

First author: JI Huali, female, born in 1989, master, mainly engaged in sedimentary basin analysis and research on metallogenic conditions of sandstone-type uranium deposits; Email: jhl19890303@163.com

Corresponding author: HE Zhongbo, male, born in 1980, senior engineer, mainly engaged in basin analysis, sandstone-type uranium deposit metallogenic conditions, metallogenic mechanism and metallogenic prediction research; Email: hzb100029@163.com

Manuscript received on: 2019-06-05; Accepted on: 2019-09-18; Edited by: LIU Zhiqiang

Doi: 10.16509/j.georeview.2020.01.004